Anal Bioanal Chem (2016) 408:2707–2715
DOI 10.1007/s00216-016-9373-7

TRENDS

Emerging scanning probe approaches to the measurement of ionic reactivity at energy storage materials

Zachary J. Barton[1] · **Joaquín Rodríguez-López**[1]

Received: 20 November 2015 / Revised: 19 January 2016 / Accepted: 27 January 2016 / Published online: 22 February 2016

Abstract Many modern energy storage technologies operate via the nominally reversible shuttling of alkali ions between an anode and a cathode capable of hosting them. The degradation process that occurs with normal usage is not yet fully understood, but emerging progress in analytical tools may help address this knowledge gap. By interrogating ionic fluxes over electrified surfaces, scanning probe methods may identify features that impact the local cyclability of a material and subsequently help inform rational electrode design for future generations of batteries. Methods developed for identifying ion fluxes for batteries show great promise for broader applications, including biological interfaces, corrosion, and catalysis.

Keywords Electroanalytical methods · Electrochemical sensors · Li-ion batteries · SECCM · SECM · SICM · Stripping analysis

Introduction to energy storage materials and ionic gradients

Enormous research efforts are focused on developing better battery electrode materials. Identifying connections between the concerted movement of ions and exchange of electrons is a fundamental challenge to battery technology development. This challenge is not unique to the field of energy storage, however, and methods developed for identifying ion fluxes at biological [1–4] and metallurgical interfaces (Fig. 1) can also be applied to energy storage. For example, a scanning electrochemical microscope (SECM) equipped with an amperometric ion-selective electrode (ISE) made from a nanopipette has been used to image K^+ channels in living kidney cells [5]. Similarly, an SECM equipped with a potentiometric ISE has been implemented to compare corrosion rates and pitting mechanisms of various Mg-containing automotive alloys [6]. Modern Li-ion batteries deliver usable current by shuttling Li^+ from a Li^+-rich anode (e.g., solid Li or graphite preloaded with Li^+) to a Li^+-poor cathode (e.g., $LiCoO_2$ or $LiFePO_4$) [7], where the insertion of Li^+ drives a change in the charge state of a transition metal [8–10]. The anode and cathode have different structures and chemical properties, but they both depend on the interfacial structures and spatially heterogeneous reactivity to cycle reversibly. Let us first consider the anode.

Graphitic materials have captured the interest of much of the scientific community looking for an inexpensive, lightweight, and comparatively stable anode. However, a number of obstacles stand in the way of accessing the full theoretical capacity of graphitic anodes (Fig. 1). Each charge cycle causes volumetric expansion in the anode as Li^+ inserts. In fact, a full charge can produce as much as a 10 % increase in volume [9]. The mechanical stress at the electrode surface associated with Li^+ insertion/de-insertion is exacerbated by the growth of the solid electrolyte interphase (SEI) [11]. The SEI is a variegated mix of solvent breakdown products and trapped metal cations [12–14]. Its formation is unavoidable, so a great deal of effort has gone into controlling its thickness [15], elasticity [16], and electrical conductivity [17, 18] so as to maintain ionic permeability [19] as well as to attenuate resistive heating, electrode

Published in the topical collection featuring *Young Investigators in Analytical and Bioanalytical Science* with guest editors S. Daunert, A. Baeumner, S. Deo, J. Ruiz Encinar, and L. Zhang.

✉ Joaquín Rodríguez-López
joaquinr@illinois.edu

[1] Department of Chemistry, University of Illinois at Urbana-Champaign, 600 South Matthews Avenue, Urbana, IL 61801, USA

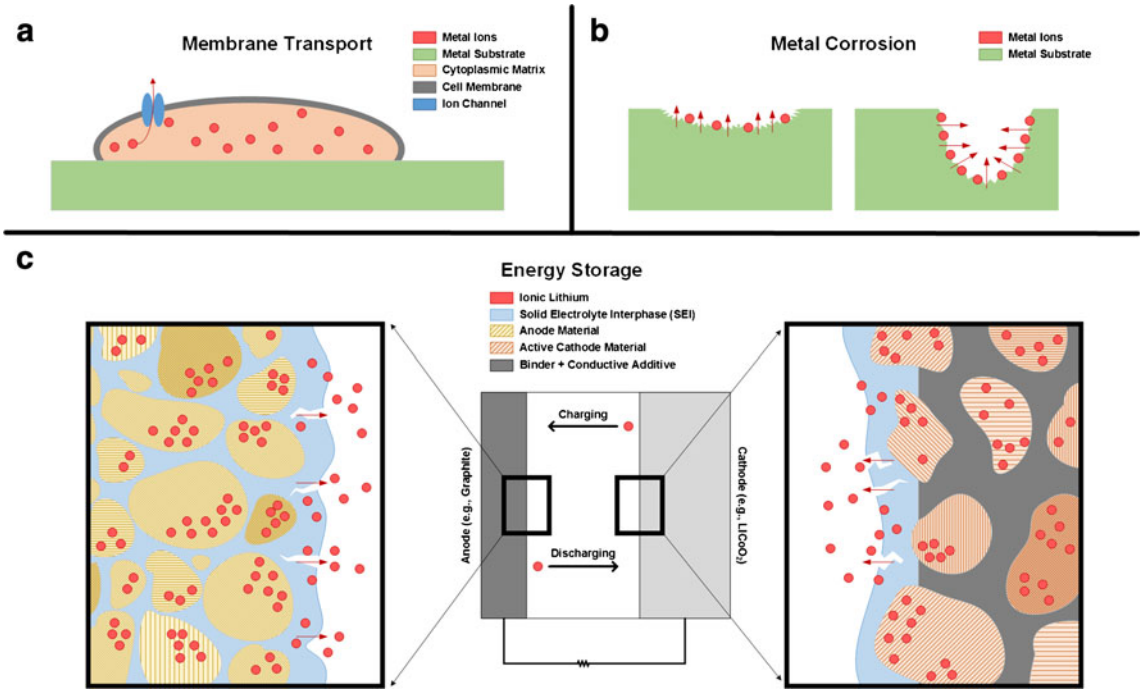

Fig. 1 Surface-based ionic processes. (**A**) Biological systems rely on a variety of ion transport systems to respond to external stimuli. (**B**) Corrosion and pitting mechanisms are highly dependent on the properties of the metal as well as the chemical environment. (**C**) Schematic of some Li-ion battery reactive heterogeneities, including volumetric strain-induced SEI damage, trapping of Li^+ in the SEI, and the formation of "hot spots" on individual particles. Exfoliation of the graphitic anode can also occur

damage, and capacity fade [20]. When properly controlled, the SEI performs an essential role in allowing anodes to operate under conditions that would otherwise destroy them.

Likewise, the presence of defect sites in the anode material is not inherently detrimental to battery performance. A wealth of evidence suggests that specific defects not only improve battery performance but also are essential to sustained operation. The accessible power density, the long term cyclability, and overall performance of a metal-ion battery hinges on the properties inherent to localized structural and chemical defects. Elaborate structures are costly, so striking a balance between engineered defects and fabrication price is vital to producing cost-effective energy storage solutions [21]. If we understood the relationships between various spatial heterogeneities and their activity, we might also be able to optimize electrode materials by engineering their microstructure. An attractive goal, then, is to isolate particular defects and study their inherent properties. However, these defects begin to appear in the first few cycles of the battery and eventually reach a saturation point [22]. The story of cycling stresses and SEI formation carries the same consequences on the cathode side of Li-ion batteries. A structural evolution of the electrode occurs during operation, so the development of defects and the SEI is best observed in situ.

The essential common feature of all modern metal ion batteries is that their operation is fundamentally tied to the movement of ions. Not surprisingly, ionic gradients are therefore a direct measure of the cyclability of a particular material. However, accessing ionic gradients in situ is not something that many analytical techniques can do. Most measurements, such as spectroscopic techniques, attempt to access ionic information indirectly through its effects. Raman spectroscopy can provide qualitative reports on the presence of defects in graphitic materials as well as changes in the plane-to-plane separation in graphene caused by Li^+ intercalation/deintercalation [22–24]. However, alkali ions themselves are Raman-silent. X-ray powder diffraction (XRD) can reveal the bulk phase composition and interplanar carbon spacing in graphite and relate them to the lithiation staging mechanism [25]. This information is also available in situ, as has been demonstrated with amorphous silicon [26]. Together with bulk electrochemical measurements, in situ XRD can provide phase diagrams of cathode materials to elucidate best practices for maximizing capacity retention [27]. X-ray photoelectron spectroscopy (XPS) can identify the presence of metals and map out their abundances and charge states, but only in a high vacuum ($<10^{-8}$ mbar) sample chamber and not while the battery is operating. Each analytical tool is useful for answering specific questions about battery operation and performance, but there are some questions that are better answered by scanning probe methods.

Introduction to electrochemical scanning probe methods

Electrochemical scanning probe methods are invaluable tools because they provide access to localized measurements of battery activity [28]. Information pertaining to the performance of individual defects is lost in bulk measurements, which average the impact of the entire electrode surface on battery performance. For example, the potential-dependent localization of Li^+ at grain boundaries in silicon can be visualized through atomic force microscopy (AFM) stress-strain measurements coupled with conductance measurements [29]. Researchers hoping to understand how the SEI impacts Li^+ diffusion [16] or how "hot spots" develop on anisotropic particles [30] need to access localized ionic measurements. Bulk measurements are well suited to assessing the viability of any particular battery as a whole but are not sufficient for designing the next generation of batteries.

The SECM was introduced by Bard et al. in 1989 for the purpose of obtaining surface maps of chemical reactivity [31–33]. An SECM consists of a potentiostat operated in conjunction with a micro- or nano-positioning system, which is used to raster a probe electrode, often a Pt, Au, or C microdisk, embedded in an insulating sheath over a substrate and coordinate reactivity to physical structures or chemically modified surface features. Over the past decade, efforts to connect surface topography to reactive heterogeneity have improved in spatial resolution as well as chemical specificity [34–39]. These emerging methods include such prominent examples as scanning ion conductance microscopy (SICM) [40, 41], scanning electrochemical cell microscopy (SECCM) [42–44], and Hg-based SECM [45–47]. General schematics of each technique are included in Fig. 2 to highlight their analytical differences as well as the rich information that can be obtained through electrochemical methods. Each technique fills its own analytical niche, and their combined progress is helping to move the field of energy storage forward. We will now consider each in turn.

Scanning ion conductance microscopy (SICM)

SICM was introduced in 1989 as a means of studying nonconducting surfaces and particularly for imaging pores in soft membranes [48]. It originally had two modes of operation: constant height and constant distance. In constant height mode, the probe was rastered through an XY plane at a preselected Z position while collecting the ionic current. On its own, constant height mode fails to decouple this ionic information from topographic effects. For example, the ionic current may decrease over a raised area of graphite even though the reactivity is unchanged. Likewise, the ionic current may decrease over a passivated area of graphite even though the substrate is flat in that area. To isolate topographic effects, SICM also had constant distance mode, wherein the probe is rastered in an XY pattern while the Z-position is modulated by a feedback loop based on the electrical conductance registered at the tip. Raised areas impinge the flow of ions through the tip's orifice, resulting in a drop in electrical conductivity and a subsequent increase in the Z-position (i.e., away from the substrate).

The first application of SICM to the nanoscale study of Li-ion batteries came in 2011 from Mark Hersam's laboratory at Northwestern University [41]. This was performed using the AC mode of SICM, in which a piezo oscillates the probe vertically during the lateral raster scans. Since the resistance between the tip and the substrate is distance-dependent, this motion generates a corresponding oscillation in the probe current. The amplitude of the oscillation serves as a feedback mechanism to correct the vertical probe position. Monitoring the ionic conductance current before and after lithiation of a 60-nm thick tin film on copper revealed the development of nanoscopic spheroidal features (via the AC component) as well as an overall boost in the ionic conductance current (via the DC component) (Fig. 3). It is worth noting that while the surface morphology changed, the contrast (relative change) in the DC current images remained unchanged, though the absolute values in the image were almost uniformly greater. This indicated that (1) the surface activity was unchanged from what it was, and (2) there were more ions present near the substrate surface than prior to lithiation. Though it is possible to speculate reasons for this, the end of the matter is that SICM needs to be coupled with supporting analytical techniques to pin down causes for the observed changes in conductivity. Hersam's group has since used SICM to confirm the success of Al_2O_3 films in preventing SEI-induced surface roughening at MnO electrodes after lithiation [49] though no attempt was made to interpret the SICM data beyond a reference to topography inferred from the AC signal.

There are now more advanced means of acquiring topographic and electrochemical information simultaneously. With respect to methodology, the latest improvement has been to approach the probe to the substrate at each XY position rather than performing an uninterrupted raster image [2]. This method greatly improves SICM's ability to track sharp changes in surface morphology and is sufficiently different from traditional SICM to warrant its own name: hopping probe ion conductance microscopy (HPICM). The reported resolution may be slightly overestimated, since recent work indicates that the fundamental limit for the lateral resolution of SICM-based methods is approximately three times the inner radius of the pipette ($3r_i$) [50]. An additional caution is the sensitivity of SICM in solutions of low ionic strength to substrate-induced charging of the nanopipette, which leads to substantial ion current rectification [51]. However, since most biological and battery environments include excess

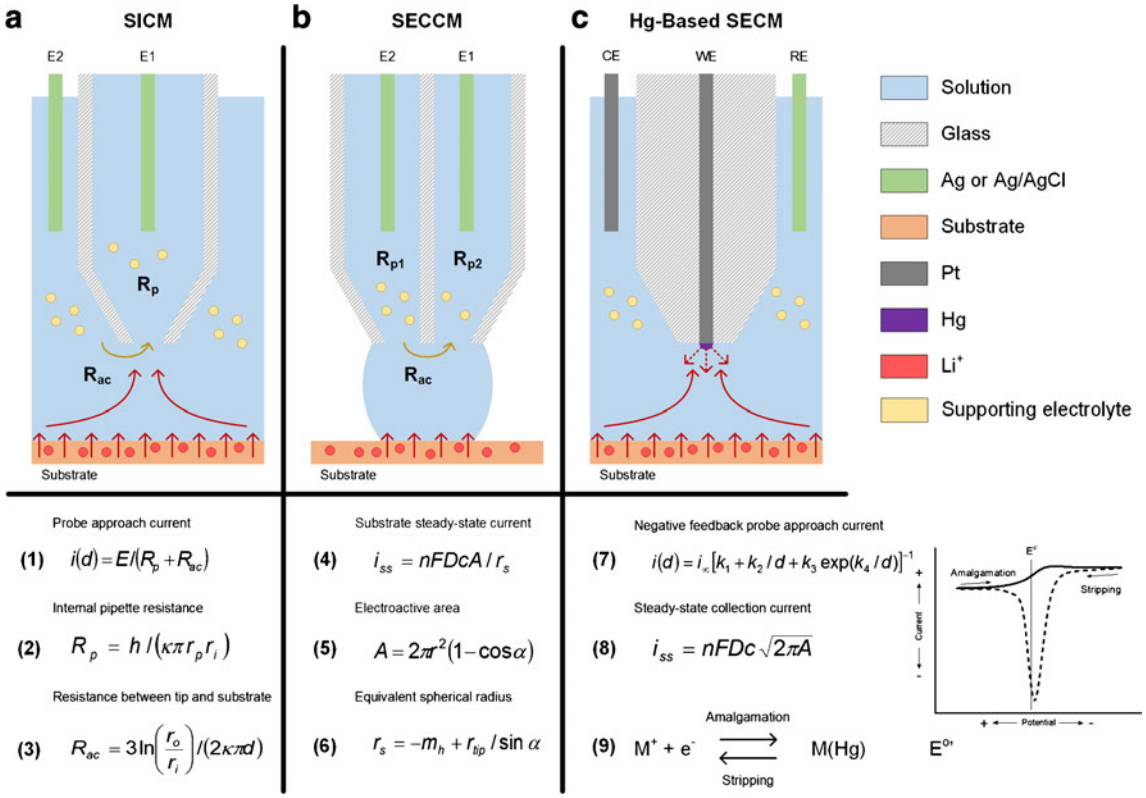

Fig. 2 Schematics of scanning probe methods discussed in this article. (**A**) The distance-dependent ionic current (*i*, Equation 1) observed at an SICM probe shares relationships with the applied potential (*E*), the internal resistance of pipette (R_p, Equation 2), and the access resistance of the solution between the probe and the substrate (R_{ac}, Equation 3). The latter two depend on the length of the tip (*h*), the conductivity of the solution (κ), the inner radius of the tip base (r_p), the inner (r_i), and outer (r_o) radius of the tip opening, and the tip-substrate gap (*d*). Topography is obtained by either hopping or oscillating the probe to pinpoint the Z-position at each XY coordinate that produces a particular preset current between the two electrodes. (**B**) After jumping to contact, the meniscus height is maintained by monitoring ionic current passing from one pipette channel to the other. When maintaining a constant tip-substrate gap, the steady-state current (i_{ss}, Equation 4) registered by the substrate working electrode depends on the number of electrons transferred (*n*), Faraday's constant (*F*), the diffusion coefficient (*D*), and concentration (*c*) of the analyte, the wetted electroactive substrate area (*A*, Equation 5), and the equivalent spherical radius of the tip (r_s, Equation 6). The electroactive substrate area is defined in terms of r_s and the half-cone angle of the tip (α), whereas r_s shares additional dependencies with the height of the meniscus (m_h) and the internal width of each pipette channel opening (r_{tip}); m_h is identical to the tip-substrate gap (*d*) only when the meniscus in contact with both the tip and the substrate. By using a dual-channel pipette, topography can be obtained by monitoring the current flowing between the two channels in the same way used for SICM. However, a major inherent benefit of SECCM is the ability to quickly relocate the substrate surface during hopping due to the absence of current before the meniscus contacts the substrate and completes the electrical circuit. (**C**) The tip-substrate gap can be monitored through negative feedback as described by Equation 7, where i_∞ is the steady-state current observed in bulk solution, *d* is the magnitude of the tip-substrate gap, and all four k_n are parameters derived from simulations. The steady-state current observed at a Hg sphere-cap SECM probe is given by Equation 8. Hg-based SECM is distinguished from SICM and SECCM by the ability to carry out stripping reactions (Equation 9) to isolate analyte signals and improve sensitivity (see inset)

supporting electrolyte, substrate-induced ion current rectification is often easily preventable.

In addition to improvements in methodology, there have also emerged bifunctional probes made from dual-barrel theta pipettes. These use a liquid channel to control position while simultaneously performing amperometric experiments at a carbon nanoelectrode in a SECM-SICM configuration [52, 53].

SICM is superbly equipped for resolving abrupt changes in surface morphology, and its ability to provide three-dimensional maps of ionic gradients through HPICM is an underutilized tool that may prove to be useful in future investigations.

Scanning electrochemical cell microscopy (SECCM)

More recently (2010), Patrick Unwin's group at the University of Warwick introduced SECCM as a tool for understanding localized heterogeneous reactivity in the context of surface features with minimal background noise [54]. The SECCM is unique in the family of scanning probe methods in that the probe contains the only electrolyte solution. Wherever the probe is brought sufficiently close to a substrate, the meniscus jumps down to contact the surface, forming a miniature electrochemical cell. Retracting and performing a jump to contact at each XY position produces a topographic map that is completely decoupled from surface electrochemical activity.

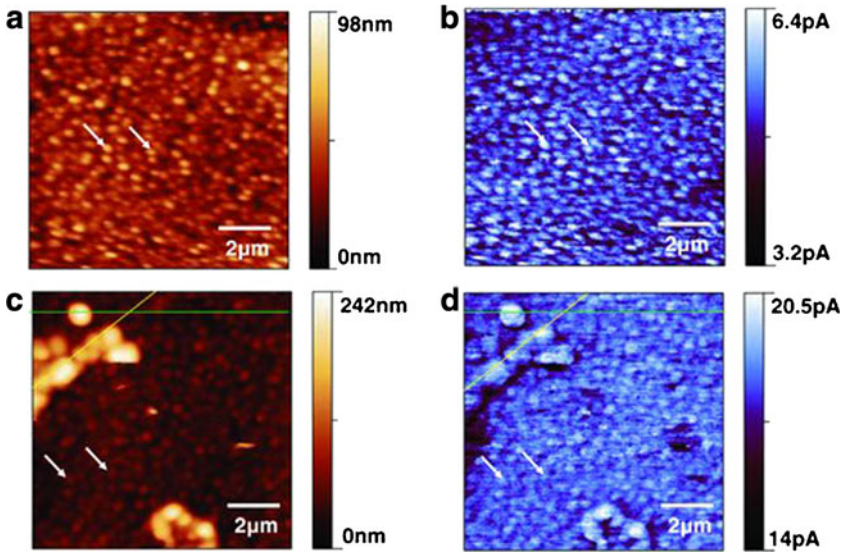

Fig. 3 SICM (**a**, **c**) topography and (**b**, **d**) DC current images of a 60 nm thick tin thin film deposited on a 60 nm thick copper thin film on glass (**a**, **b**) before lithiation and (**c**, **d**) after 24 μAh cm^{-2} lithiation. Reproduced from Lipson et al. [41] with permission

However, the true power of SECCM is revealed in studies of electroactive substrates. When connected as the working electrode, the substrate current is inherently free from much of the background noise and capacitance associated with large electrodes because only a small region is activated at any given time. This was demonstrated over a cathode material ($LiFePO_4$) for aqueous Li-ion batteries in 2014, when a collaborative effort reported by Takahashi et al. [43] created maps of topography combined with surface deintercalation activity (Fig. 4). The greatly improved signal-to-noise ratio of SECCM compared with SICM allows for the execution of localized charge and discharge curves as well as galvanostatic time-resolved potential mapping.

Unwin's group has gone on to report the development of quad-barrel SECCM-SECM probes [55]. Though these probes have yet to be applied to energy storage materials or used in organic solvents, they show great promise as aqueous probes.

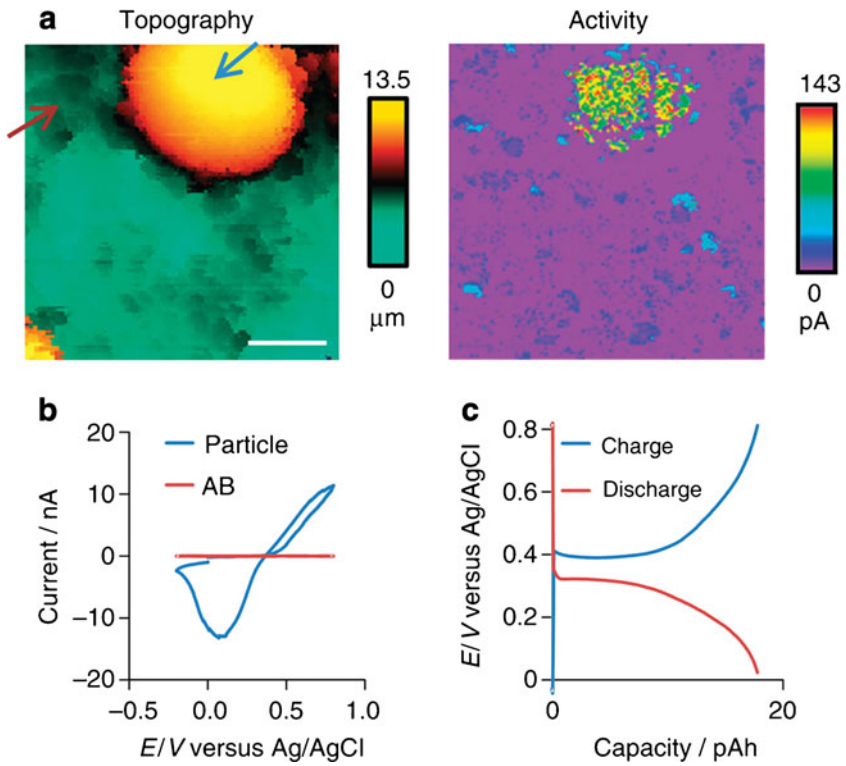

Fig. 4 (**a**) Simultaneous SECCM topography (left) and current (right) images. Scan ranges are 20 × 20 μm. The substrate potential was +0.65 V versus Ag/AgCl QRCE (Li^+ deintercalation; scale bar, 5 μm). (**b**) CVs at different points on a $LiFePO_4$ electrode surface, corresponding to the blue and red arrow of a. Scan rate is 0.1 V s^{-1}. (**c**) Local charge (deintercalation) and discharge (intercalation) characteristics applying current magnitudes of 200 pA in each case via SECCM. Reproduced from Takahashi et al. [43] with permission

Though the absence of bulk solvent contact with the substrate provides localized measurements with superb signal-to-noise ratios, a possible criticism of SECCM is that this very same absence prevents representative operating conditions. The composition of the SEI is dependent on cycling history, both for electrochemical and physical reasons. The depth to which the electrode is cycled impacts the staging mechanism for Li intercalation. For example, some Li is consumed by solvent breakdown products at the electrode surface in ways that change over time and with each cycle. Furthermore, the mechanical surface strains placed on the electrode by changes in volume may have a lateral component [30]. There may be many things worth learning from SECCM, but representative SEI behavior may be difficult to access in a traveling cell method. Nevertheless, the unprecedented signal-to-noise ratios gained from miniaturization of the electrochemical cell and the inherent separation of topography and electrochemical activity through jump-to-contact positioning of the probe ensure that SECCM will remain at the forefront of future investigations of ionic fluxes.

Hg-based scanning electrochemical microscopy (SECM)

Hg-functionalized microelectrodes surfaced in the 1980s [56], predating even the birth of SECM. However, their use as SECM probes was not reported until the early 2000s [57, 58]. Hg-based SECM allows for multiple working electrodes and has been shown to operate in both aqueous [46] and non-aqueous conditions, unlike SICM, which has only been shown to operate under aqueous conditions. SECCM has been shown to operate also in an ionic liquid [59] but has yet to be employed in a typical energy storage environment. Recently, Hg-based SECM was used in the redox competition mode to differentiate between a Au electrode and PTFE on the basis of Li^+ gradients in propylene carbonate as a proxy for battery environments (Fig. 5) [47]. In this configuration, both the Hg-based probe and the conductive substrate are poised at potentials to reduce Li^+ from solution. This platform differs from SICM and SECCM in that the current registered by the probe is a direct measure of the local Li^+ concentration and not of other ions.

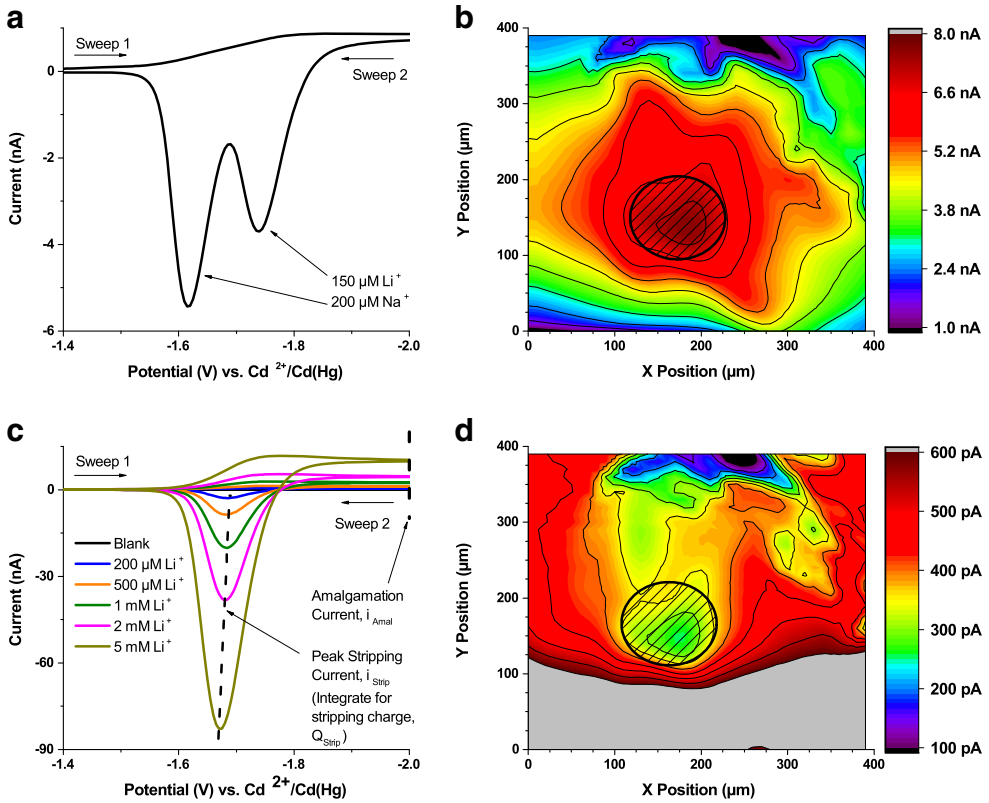

Fig. 5 Stripping voltammetry (**A**, **C**) of alkali ions in PC by Hg-capped Pt UMEs and SECM images (**B**, **D**) over a 120 μm diameter Au electrode (outlined in black). **A**: Experimental CV of 150 μM Li^+, 200 μM Na^+, and 100 mM TBAP in PC. The current is offset by –400 pA to account for background current. **C**: Representative CVs of $LiClO_4$ and 100 mM TBAP in PC. Integration of the peak stripping current gives the stripping charge. All $\nu = 100$ mV s^{-1}. **B**: SECM image of ethyl viologen feedback. An increase in redness indicates an increase in substrate activity. **D**: SECM image of Li^+ consumption using redox competition mode. Lithium flux at the tip ($E_{Tip} = -2.87$ V) responded to activation of the substrate toward lithium reduction ($E_{Sub} = -3.0$ V). An increase in blueness indicates a decrease in free Li^+ concentration. Adapted from Barton and Rodríguez-López [47]

In fact, a further benefit of Hg-based probes is the ability to perform stripping voltammetry. The stripping signal is useful because (1) the ability to preconcentrate ions and increase signal strength allows rapid measurements and promotes high signal-to-noise ratios, which are a distinct concern with nanoscale SICM current measurements [4], and (2) many metal ions can be differentiated by their signature stripping potential, thereby allowing the simultaneous analysis of multiple metal ions (Fig. 5). This may become useful in studies of cathode materials, since leaching of metals from the cathode is a known issue [60]. The stripping signal from Hg-based probes has been used for rapid, multi-ion-specific imaging of heavy metals in aqueous solutions before [45], and will soon be reported for alkali metals in nonaqueous solvents by our own laboratory. SICM and SECCM are readily able to decouple topographical and electrochemical information, but they lack the inherent chemical specificity available to Hg-based SECM.

Hg-based SECM investigations are reported with resolutions (3 μm [45] and 10 μm [47]) that do not yet match those offered by SICM (30 nm [41]) or SECCM (100 nm [43]), but this does not mean that nanoscale resolution is unattainable with these probes. In fact, we have already demonstrated [47] the feasibility of miniaturization through Hg-functionalized pyrolyzed carbon-based nanopipettes [61, 62].

Though most SECM experiments are still executed in constant height mode, which does not differentiate between changes in the current caused by topography or by electrochemical activity, there are already some reported methods for operating in constant distance mode. These include shear force [63], AC impedance [64], and hopping intermittent contact [65]. As Hg-based SECM follows the inexorable march of scanning probe techniques towards nanoscale measurements, it may also adopt these or newer methods for separating surface morphology from reactivity.

Outlook

Electrochemical microscopy draws from advanced concepts in charge transfer and ionic conductivity to achieve the imaging of ionic phenomena at battery interfaces. Coupling electrode surface morphology to electrochemical information reveals important relationships that are otherwise difficult to access. In this brief Trends article, we have highlighted three emerging electrochemical scanning probe techniques that achieve this. SICM is able to resolve abrupt changes in surface topography, SECCM supports high signal-to-noise measurements, and Hg-based SECM permits the collection of ionic signals with chemical specificity. The story is well advanced for Li-ion batteries, but many questions remain to be answered for Na-ion and K-ion batteries [66]. Since we are just beginning to understand what happens under sodiation and desodiation [67, 68], ion-sensitive scanning probe methods have the potential to make valuable contributions to the development of the next generation of energy storage technologies. These developments will have a broad impact on our ability to address a diversity of interfaces in other fields, such as biology and corrosion science, where understanding ion transport and reactivity at the nanoscale is also essential for understanding function.

Acknowledgements Z.J.B. acknowledges the support of the National Science Foundation Graduate Research Fellowship Program (DGE-1144245). Any opinions, findings, and conclusions or recommendations expressed in this material are those of the authors and do not necessarily reflect the views of the National Science Foundation. J. R.-L. acknowledges support from the Joint Center for Energy Storage Research, an Energy Innovation Hub funded by the US Department of Energy, Office of Science, Basic Energy Sciences. The authors also thank UIUC for generous start-up funds.

Compliance with ethical standards

Conflict of Interest The authors declare no conflict of interest.

References

1. Scott ER, White HS, Phipps JB. Iontophoretic transport through porous membranes using scanning electrochemical microscopy: application to in vitro studies of ion fluxes through skin. Anal Chem. 1993;65(11):1537–45.
2. Novak P, Li C, Shevchuk AI, Stepanyan R, Caldwell M, Hughes S, et al. Nanoscale live-cell imaging using hopping probe ion conductance microscopy. Nat Methods. 2009;6(4):279–81.
3. Shen M, Ishimatsu R, Kim J, Amemiya S. Quantitative imaging of ion transport through single nanopores by high-resolution scanning electrochemical microscopy. J Am Chem Soc. 2012;134(24):9856–9.
4. Chen C-C, Zhou Y, Morris CA, Hou J, Baker LA. Scanning ion conductance microscopy measurement of paracellular channel conductance in tight junctions. Anal Chem. 2013;85(7):3621–8.
5. Yamada H, Haraguchi D, Yasunaga K. Fabrication and characterization of a K^+-selective nanoelectrode and simultaneous imaging of topography and local K^+ flux using scanning electrochemical microscopy. Anal Chem. 2014;86(17):8547–52.
6. Dauphin-Ducharme P, Asmussen RM, Shoesmith DW, Mauzeroll J. In-situ Mg^{2+} release monitored during magnesium alloy corrosion. J Electroanal Chem. 2015;736(C):61–8.
7. Kang B, Ceder G. Battery materials for ultrafast charging and discharging. Nature. 2009;458(7235):190–3.
8. Goodenough JB, Kim Y. Challenges for rechargeable Li batteries. Chem Mater. 2010;22(3):587–603.
9. Etacheri V, Marom R, Elazari R, Salitra G, Aurbach D. Challenges in the development of advanced Li-ion batteries: a review. Energy Environ Sci. 2011;4(9):3243–62.
10. Goodenough JB, Park K-S. The Li-ion rechargeable battery: a perspective. J Am Chem Soc. 2013;135(4):1167–76.
11. Tavassol H, Chan MKY, Catarello MG, Greeley JP, Cahill DG, Gewirth AA. Surface coverage and SEI induced electrochemical surface stress changes during Li deposition in a model system for Li-ion battery anodes. J Electrochem Soc. 2013;160(6):A888–96.

12. Aurbach D, Daroux ML, Faguy PW, Yeager E. Identification of surface films formed on lithium in propylene carbonate solutions. J Electrochem Soc. 1987;134(7):1611–20.
13. Verma P, Maire P, Novák P. A review of the features and analyses of the solid electrolyte interphase in Li-ion batteries. Electrochim Acta. 2010;55(22):6332–41.
14. Norberg NS, Lux SF, Kostecki R. Interfacial side-reactions at a $LiNi_{0.5}Mn_{1.5}O_4$ electrode in organic carbonate-based electrolytes. Electrochem Commun. 2013;34(C):29–32.
15. Smith AJ, Burns JC, Zhao X, Xiong D, Dahn JR. A high precision coulometry study of the SEI growth in Li/graphite cells. J Electrochem Soc. 2011;158(5):A447–52.
16. Aurbach D. Review of selected electrode–solution interactions which determine the performance of Li and Li ion batteries. J Power Sources. 2000;89(2):206–18.
17. Petibon R, Sinha NN, Burns JC, Aiken CP, Ye H, VanElzen CM, et al. Comparative study of electrolyte additives using electrochemical impedance spectroscopy on symmetric cells. J Power Sources. 2014;251:187–94.
18. Wang DY, Sinha NN, Burns JC, Petibon R, Dahn JR. A high precision study of the electrolyte additives vinylene carbonate, vinyl ethylene carbonate and lithium bis(oxalate)borate in $LiCoO_2$/graphite pouch cells. J Power Sources. 2014;270:68–78.
19. Persson K, Sethuraman VA, Hardwick LJ, Hinuma Y, Meng YS, van der Ven A, et al. Lithium diffusion in graphitic carbon. J Phys Chem Lett. 2010;1(8):1176–80.
20. Zheng J, Gu M, Xiao J, Zuo P, Wang C, Zhang J-G. Corrosion/fragmentation of layered composite cathode and related capacity/voltage fading during cycling process. Nano Lett. 2013;13(8):3824–30.
21. Darling RM, Gallagher KG, Kowalski JA, Ha S, Brushett FR. Pathways to low-cost electrochemical energy storage: a comparison of aqueous and nonaqueous flow batteries. Energy Environ Sci. 2014;7:3459–77.
22. Jaber-Ansari L, Puntambekar KP, Tavassol H, Yildirim H, Kinaci A, Kumar R, et al. Defect evolution in graphene upon electrochemical lithiation. ACS Appl Mater Interfaces. 2014;6(20):17626–36.
23. Inaba M, Yoshida H, Ogumi Z, Abe T, Mizutani Y, Asano M. In Situ Raman study on electrochemical Li intercalation into graphite. J Electrochem Soc. 1995;142(1):20–6.
24. Sole C, Drewett NE, Hardwick LJ. In situ Raman study of lithium-ion intercalation into microcrystalline graphite. Faraday Discuss. 2014;172:223–37.
25. Dahn JR. Phase diagram of Li_xC_6. Phys Rev B. 1991;44(17):9170–7.
26. Hatchard TD, Dahn JR. In situ XRD and electrochemical study of the reaction of lithium with amorphous silicon. J Electrochem Soc. 2004;151(6):A838–42.
27. Chen Z, Dahn JR. Methods to obtain excellent capacity retention in $LiCoO_2$ cycled to 4.5 V. Electrochim Acta. 2004;49(7):1079–90.
28. Lipson AL, Hersam MC. Conductive scanning probe characterization and nanopatterning of electronic and energy materials. J Phys Chem C. 2013;117(16):7953–63.
29. Balke N, Jesse S, Kim Y, Adamczyk L, Tselev A, Ivanov IN, et al. Real space mapping of Li-ion transport in amorphous Si anodes with nanometer resolution. Nano Lett. 2010;10(9):3420–5.
30. Harris SJ, Lu P. Effects of inhomogeneities—nanoscale to mesoscale—on the durability of Li-ion batteries. J Phys Chem C. 2013;117(13):6481–92.
31. Bard AJ, Fan F-R, Kwak J, Lev O. Scanning electrochemical microscopy. Introduction and principles. Anal Chem. 1989;61(2):132–8.
32. Bard AJ, Denuault G, Lee C, Mandler D, Wipf DO. Scanning electrochemical microscopy—a new technique for the characterization and modification of surfaces. Acc Chem Res. 1990;23(11):357–63.
33. Bard AJ, Fan F-R, Pierce DT, Unwin PR, Wipf DO, Zhou F. Chemical imaging of surfaces with the scanning electrochemical microscope. Science. 1991;254:68–74.
34. Sun P, Laforge FO, Mirkin MV. Scanning electrochemical microscopy in the 21st century. Phys Chem Chem Phys. 2007;9(7):802–23.
35. Bertoncello P. Advances on scanning electrochemical microscopy (SECM) for energy. Energy Environ Sci. 2010;3(11):1620–33.
36. Mirkin MV, Nogala W, Velmurugan J, Wang Y. Scanning electrochemical microscopy in the 21st century. Update 1: 5 years after. Phys Chem Chem Phys. 2011;13(48):21196–212.
37. Kranz C. Recent advancements in nanoelectrodes and nanopipettes used in combined scanning electrochemical microscopy techniques. Analyst. 2014;139(2):336–52.
38. Bülter H, Peters F, Schwenzel J, Wittstock G. Spatiotemporal changes of the solid electrolyte interphase in lithium-ion batteries detected by scanning electrochemical microscopy. Angew Chem Int Ed. 2014;53(39):10531–5.
39. Ventosa E, Schuhmann W. Scanning electrochemical microscopy of Li-ion batteries. Phys Chem Chem Phys. 2015;17:28441–50.
40. Chen C-C, Zhou Y, Baker LA. Scanning ion conductance microscopy. Annu Rev Anal Chem. 2012;5(1):207–28.
41. Lipson AL, Ginder RS, Hersam MC. Nanoscale in situ characterization of Li-ion battery electrochemistry via scanning ion conductance microscopy. Adv Mater. 2011;23(47):5613–7.
42. Ebejer N, Güell AG, Lai SCS, McKelvey K, Snowden ME, Unwin PR. Scanning electrochemical cell microscopy: a versatile technique for nanoscale electrochemistry and functional imaging. Annu Rev Anal Chem. 2013;6(1):329–51.
43. Takahashi Y, Kumatani A, Munakata H, Inomata H, Ito K, Ino K, et al. Nanoscale visualization of redox activity at lithium-ion battery cathodes. Nat Commun. 2014;5:1–7.
44. Momotenko D, Byers JC, McKelvey K, Kang M, Unwin PR. High-speed electrochemical imaging. ACS Nano. 2015;9(9):8942–52.
45. Alpuche-Aviles M, Baur JE, Wipf DO. Imaging of metal ion dissolution and electrodeposition by anodic stripping voltammetry-scanning electrochemical microscopy. Anal Chem. 2008;80(10):3612–21.
46. Souto RM, González-García Y, Battistel D, Daniele S. In situ scanning electrochemical microscopy (SECM) detection of metal dissolution during zinc corrosion by means of mercury sphere-cap microelectrode tips. Chem Eur J. 2011;18(1):230–6.
47. Barton ZJ, Rodríguez-López J. Lithium ion quantification using mercury amalgams as *in situ* electrochemical probes in nonaqueous media. Anal Chem. 2014;86(21):10660–7.
48. Hansma P, Drake B, Marti O, Gould S, Prater C. The scanning ion-conductance microscope. Science. 1989;243(4891):641–3.
49. Lipson AL, Puntambekar K, Comstock DJ, Meng X, Geier ML, Elam JW, et al. Nanoscale investigation of solid electrolyte interphase inhibition on Li-ion battery MnO electrodes via atomic layer deposition of Al_2O_3. Chem Mater. 2014;26(2):935–40.
50. Rheinlaender J, Schäffer TE. Lateral resolution and image formation in scanning ion conductance microscopy. Anal Chem. 2015;87(14):7117–24.
51. Sa N, Lan W-J, Shi W, Baker LA. Rectification of Ion current in nanopipettes by external substrates. ACS Nano. 2013;7(12):11272–82.
52. Takahashi Y, Shevchuk AI, Novak P, Zhang Y, Ebejer N, Macpherson JV, et al. Multifunctional nanoprobes for nanoscale chemical imaging and localized chemical delivery at surfaces and interfaces. Angew Chem Int Ed. 2011;50(41):9638–42.
53. O'Connell MA, Wain AJ. Mapping electroactivity at individual catalytic nanostructures using high-resolution scanning electrochemical-scanning ion conductance microcopy. Anal Chem. 2014;86(24):12100–7.

54. Ebejer N, Schnippering M, Colburn AW, Edwards MA, Unwin PR. Localized high resolution electrochemistry and multifunctional imaging: scanning electrochemical cell microscopy. Anal Chem. 2010;82(22):9141–5.
55. Paulose Nadappuram B, McKelvey K, Byers JC, Güell AG, Colburn AW, Lazenby RA, et al. Quad-barrel multifunctional electrochemical and ion conductance probe for voltammetric analysis and imaging. Anal Chem. 2015;87(7):3566–73.
56. Wehmeyer KR, Wightman RM. Cyclic voltammetry and anodic stripping voltammetry with mercury ultramicroelectrodes. Anal Chem. 1985;57(9):1989–93.
57. Selzer Y, Mandler D. Scanning electrochemical microscopy. Theory of the feedback mode for hemispherical ultramicroelectrodes: steady-state and transient behavior. Anal Chem. 2000;2(11):2383–90.
58. Mauzeroll J, Hueske EA, Bard AJ. Scanning electrochemical microscopy. 48. Hg/Pt hemispherical ultramicroelectrodes: fabrication and characterization. Anal Chem. 2003;75(15):3880–9.
59. Aaronson BDB, Byers JC, Colburn AW, McKelvey K, Unwin PR. Scanning electrochemical cell microscopy platform for ultrasensitive photoelectrochemical imaging. Anal Chem. 2015;87(8):4129–33.
60. Danis L, Gateman SM, Snowden ME, Halalay IC, Howe JY, Mauzeroll J. Anodic stripping voltammetry at nanoelectrodes: trapping of Mn^{2+} by crown ethers. Electrochim Acta. 2015;162:169–75.
61. Singhal R, Bhattacharyya S, Orynbayeva Z, Vitol E, Friedman G, Gogotsi Y. Small diameter carbon nanopipettes. Nanotechnology. 2009;21(1):015304.
62. Actis P, Tokar S, Clausmeyer J, Babakinejad B, Mikhaleva S, Cornut R, et al. Electrochemical nanoprobes for single-cell analysis. ACS Nano. 2014;8(1):875–84.
63. Danis L, Snowden ME, Tefashe UM, Heinemann CN, Mauzeroll J. Development of nano-disc electrodes for application as shear force sensitive electrochemical probes. Electrochim Acta. 2014;136:121–9.
64. Alpuche-Aviles M, Wipf DO. Impedance feedback control for scanning electrochemical microscopy. Anal Chem. 2001;73(20):4873–81.
65. Lazenby RA, McKelvey K, Unwin PR. Hopping intermittent contact-scanning electrochemical microscopy (HIC-SECM): visualizing interfacial reactions and fluxes from surfaces to bulk solution. Anal Chem. 2013;85(5):2937–44.
66. Luo W, Wan J, Ozdemir B, Bao W, Chen Y, Dai J, et al. Potassium ion batteries with graphitic materials. Nano Lett. 2015;15(11):7671–7.
67. Gu M, Kushima A, Shao Y, Zhang J-G, Liu J, Browning ND, et al. Probing the failure mechanism of SnO_2 nanowires for sodium-ion batteries. Nano Lett. 2013;13(11):5203–11.
68. Islam MS, Fisher CAJ. Lithium and sodium battery cathode materials: computational insights into voltage, diffusion, and nanostructural properties. Chem Soc Rev. 2013;43(1):185–204.